JOURNAL OF CATALYSIS 147, 115–122 (1994)

Characterisation of Chromium Ion-Doped Titania by FTIR and XPS

A. M. Venezia,* L. Palmisano,† M. Schiavello,‡ C.Martin,§ I. Martin,§ and V. Rives§,[1]

*CNR-ICTPN, c/o Dipartimento di Chimica Inorganica, Università di Palermo, Italy; †Dipartimento di Chimica, Università della Calabria, 87030 Arcavacata di Rende, Cs, Italy; ‡Dipartimento di Ingegneria Chimica dei Processi e dei Materiali, Università di Palermo, Italy; §Departamento de Química Inorgánica, Universidad de Salamanca, Facultad de Farmacia, 37007-Salamanca, Spain

Received April 20, 1993; revised October 15, 1993

Chromium ion-doped polycrystalline titania catalysts, mainly used in photoreactions, were studied by Fourier transform infrared (FTIR) spectroscopy and by X-ray photoelectron spectroscopy (XPS). Two series of catalysts prepared by two different methods, i.e., coprecipitation and impregnation, were analysed. The FTIR spectra recorded upon adsorption of ammonia and after outgassing at increasing temperatures indicated that Cr_xO_y/TiO_2 samples, whichever preparation method was used, have two types of surface acid sites, Lewis and Brønsted sites. The Brønsted sites are associated with the presence of chromium, since they were not detected in pure titania. According to the X-ray photoelectron study, Cr(III) and Cr(VI) species are present in both series of catalysts, with the higher oxidation state being quite unstable under X-rays. As shown by quantitative XPS analysis, only the catalysts prepared by coprecipitation and containing up to 2% Cr can be described by the Kerkhof–Moulijn monolayer model. © 1994 Academic Press, Inc.

INTRODUCTION

The system formed by Chromium-doped polycrystalline titania has been widely studied in the field of photocatalysis (1); in particular it has been used for dinitrogen photoreduction to NH_3 and for phenol photodegradation in the gas–solid and in the liquid–solid regimes, respectively.

Doping with Cr(III) ions has been found essential for the occurrence of dinitrogen photoreduction in the gas–solid regime and ineffectual or detrimental, depending on the amount, for phenol photodegradation in aqueous dispersion (2). The role of Cr(III) ions used as dopant for TiO_2 is mainly to improve the charge separation of the photoproduced hole-electron pairs by means of a permanent electric field.

The system was also structurally investigated using different techniques, like X-ray diffraction, BET, SEM, etc. (1, 2), although an exhaustive investigation has not been made. Consequently, additional information concerning the surface element distribution, chemical states, and acidity could be helpful for a better understanding of the photocatalytic behaviour.

The present study is aimed at determining the surface distribution of Cr ions on titania by using the XPS technique, which is a powerful tool for the determination of the surface element distributions and chemical states. Information on surface acidity, as measured by FTIR spectroscopy monitoring of ammonia adsorption, is also included, in order to complete previous studies carried out with the same technique, applied to adsorption of pyridine (3).

EXPERIMENTAL

Two series of catalysts were prepared; one set was prepared by impregnation (4) and the other by coprecipitation (2). The former catalysts are designated as TC-IM and the latter as TC-CP, followed by a number indicating the nominal Cr content (at%). TC-IM samples (Cr/Ti = 1, 3, and 5 at%) were obtained by impregnating TiO_2 (Degussa P25, bulk density $\rho = 4.18$ g cm^{-3}, specific surface area $S_O = 49$ m^2 g^{-1}), heated overnight at 670 K to eliminate adsorbed organic residues, with an aqueous solution (50 ml) containing desired amounts of CrO_3 (U.C.B., Belgium). After stirring for 60 min, the solvent was slowly evaporated at 330 K and the samples were dried overnight at 380 K. The yellow powder obtained was heated for 3 h at 770 K in oxygen flow and then was cooled to room temperature for 16 h. This last procedure produced a major reduction of Cr(VI) to Cr(III) (4).

TC-CP samples (Cr/Ti = 0.2, 0.5, 1.0, 2.0, and 5.0 at%) were obtained by reacting aqueous solutions of $TiCl_3$ (15 wt% Carlo Erba) containing the required amount of Cr(III) ions (e.g., $Cr(NO_3)_3 \cdot 9H_2O$, Merck) with aqueous solutions of ammonia (25 wt% Merck). The solids were filtered, washed, and then left standing for 24 h at room temperature. Then they were dried at 393 K for 24 h and finally fired in air for 24 h at 773 K. Pure "home prepared" TiO_2(hp) ($\rho = 3.84$ g cm^{-3}, $S_O = 51$ m^2 g^{-1}) was obtained following a procedure similar to the method used for the TC-CP catalysts.

[1] To whom correspondence should be addressed.

0021-9517/94 $6.00

The majority of the particle sizes were in the range 500–1500 nm and 100–300 nm as determined by scanning electron microscopy (2).

The Fourier transform infrared (FTIR) spectra were recorded in a 16-PC Perkin–Elmer spectrometer (nominal resolution 2 cm^{-1}, averaging 100 scans). A special Pyrex cell that allows recording of the spectra in vacuum or under a controlled atmosphere was used. The procedure was performed as follows: the solid was compacted to a self-supported disc (1 cm diameter) weighing 50–60 mg and was calcined at 673 K for 2 h in the cell in order to eliminate any organic impurities adsorbed during the preparation. The sample was outgassed at 673 K for 2 h at a residual pressure of ca. 10^{-3} N m^{-2}, and, after cooling to room temperature, it was equilibrated with ammonia (20 mbar) and then outgassed for 30 min by increasing the temperatures to 673 K. The spectra of the solid were subtracted using the software utilities provided by the spectrometer. Only the 1700–1100 cm^{-1} range is shown in the figures, as this is where the bands due to vibrational modes of adsorbed ammonia are expected to be recorded.

The XPS analysis was performed with a VG ESCALAB MKII spectrometer. The X-ray source was Al$K\alpha$ (1486.6 eV) run at 20 mA and 15 kV. The spectra were obtained in the digital mode (VGS 1000 software on an Apple IIe). The spherical sector analyzer operated in the fixed analyzer transmission (FAT) mode with a pass energy of 20 eV set across the hemispheres. The instrument was calibrated according to (5). The residual pressure in the spectrometer during data acquisition was lower than 5×10^{-7} N m^{-2}. The samples were analysed as powder dusted on a double-sided adhesive tape.

The spectra were resolved into their Gaussian–Lorentzian components after background subtraction following the method of Shirley (6) and Sherwood (7). The energies and the areas of the peaks were calculated with a nonlinear least-squares procedure. The full widths at half maximum (FWHM) were allowed to change to attain the best fitting. The binding energies were referred to the binding energy of the contamination carbon (1*s*) peak at 285.0 eV. The values reported here are the average of at least two measurements, whose reproducibility was ±0.1 eV. The intensity ratios were obtained by the peak area ratios divided by the element sensitivity factors, calculated with the cross sections by Scofield (8) and with the asymmetry function (9).

RESULTS AND DISCUSSION

FTIR Assessment of Surface Acidity

The spectra recorded for the unloaded supports, TiO_2 hp and P25, are shown in Fig. 1. For support P25 (Fig. 1e) the bands recorded upon adsorption of ammonia are

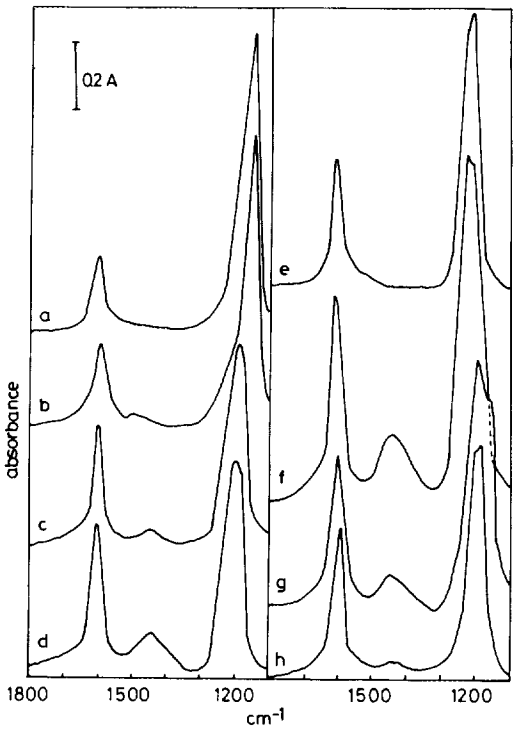

FIG. 1. FTIR spectra recorded upon adsorption of ammonia at room temperature and outgassing at room temperature on supports (a) hp and (e) P25, and on samples (b) TC-CP0.2 and TC-CP0.5; (c) TC-CP3, (d) TC-CP5, (f) TC-IM5, (g) TC-IM3, and (h) TC-IM1.

located at 1603 and 1190 cm^{-1}, and are respectively ascribed to δ_{as} and δ_s modes of NH_3 molecularly adsorbed on surface Lewis acid sites. The splitting observed for the δ_s band has been previously reported by Busca *et al.* (10), and indicates the presence of two types of surface acid sites. The weaker ones, β-sites, corresponding to five-coordinated (C_{4v}) exposed Ti^{4+} species, are responsible for the band at 1185 cm^{-1}, which disappears upon outgassing the sample at low temperature, and the stronger surface Lewis acid sites, α-sites, corresponding to Ti^{4+} ions in C_{2v} coordination, which are responsible for the band at 1229 cm^{-1}. Upon outgassing at increasing temperatures the band due to adsorption on β-sites is removed more easily than that due to adsorption on α-sites.

For the hp support, under the same conditions as for TiO_2 P-25 (Fig. 1a), the bands are recorded at 1603 and 1150 cm^{-1}, corresponding to the δ_{as} and δ_s modes. No splitting of the δ_s band is observed, indicating that all exposed surface Lewis acid sites are of the β-type (weak). The intensities of the bands slightly decrease upon outgassing at increasing temperatures, with a simultaneous splitting and shift of the δ_s band to 1230 and 1200 cm^{-1} when the sample is outgassed at 573 K. The bands are completely removed upon outgassing at 673 K.

The spectra recorded upon adsorption and outgassing at room temperature of ammonia on samples TC-CP0.2 and TC-CP0.5 are coincident, and are shown in Fig. 1b. They are very similar to that for parent support hp, although in addition to the bands described above, a weak band at 1484 cm^{-1} is also recorded, which can be ascribed to the presence of NH_2 species through dissociative adsorption of NH_3. As will be shown in Fig. 2, for the TC-CP0.2 sample, on outgassing at room temperature this band almost vanishes, while the behaviour observed for the other bands follows the same trend observed for the support.

When the chromium content is increased (samples TC-CP3 and TC-CP5, Figs. 1c and 1d), the spectra are very similar, with an intense band at 1603 cm^{-1} and a broad band at 1190–1210 cm^{-1} which correspond to the asymmetric and symmetric modes of ammonia chemisorbed on surface Lewis acid sites. Unfortunately, the bands corresponding to adsorption on surface Lewis acid sites originated by coordinatively unsaturated Ti^{4+} or Cr^{3+} ions are recorded in positions too close to be unambiguously distinguished. In addition, a new band, not observed upon adsorption of ammonia on the support or on the low-loaded samples, is observed at 1446 cm^{-1}. This band has been ascribed to the asymmetric deformation mode of ammonium species, NH_4^+, thus suggesting that incorporation of appreciable amounts of chromium leads to the formation of surface Brønsted acid sites (Cr^{6+}–OH), whose concentration increases with the chromium content. Surface acid Brønsted sites are associated to chromium ions in a high oxidation state, while surface Lewis sites are associated to Cr(III) species, which correlates with literature data for bulk Cr_2O_3 and CrO_3 (11).

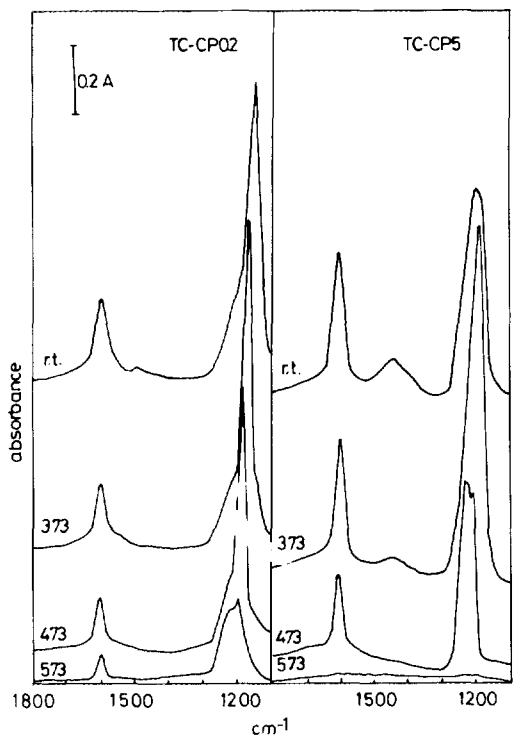

FIG. 2. FTIR spectra recorded upon adsorption of ammonia at room temperature on samples TC-CP0.2 and TC-CP5, and outgassing for 30 min at the temperatures given (K).

Both types of adsorbed ammonia–ammonium species behave differently when the sample is outgassed at increasing temperatures (Fig. 2). The outgassing temperature required to remove the band associated to the presence of NH_4^+ species (ammonia adsorbed on surface Brønsted acid sites) is lower than that required to remove ammonia adsorbed on surface Lewis acid sites, indicating that these are stronger than the former ones. On the other hand, it can also be observed that when the outgassing temperature is increased a split in the low wavenumbers band is attained, its origin being probably the existence of ammonia molecules adsorbed on Lewis acid sites with a different strength. If the spectra recorded for samples TC-CP with different chromium content are compared (Fig. 2) it can be observed that as the chromium content is increased, the outgassing temperature required to remove completely adsorbed ammonia is decreased.

In a way similar to that observed for the other samples, adsorption of ammonia on samples TC-IM gives rise to spectra with bands at 1603 and 1210–1190 cm^{-1} (Figs. 1f–1h) and, in the case of sample TC-IM3 (Fig. 1g), a weak band at 1160 cm^{-1} is also recorded. All these bands are due to deformation modes of ammonia coordinated to surface Lewis acid sites. The splitting observed for the band corresponding to the δ_s mode, as already reported for the spectrum corresponding to support P25, indicates the presence of two different types of Lewis acid sites, probably associated here to Ti^{4+} and Cr^{3+} ions in different coordination environments. Surface Brønsted acid sites should be responsible for the band at 1446 cm^{-1}, ascribed to deformation mode of NH_4^+ species. As with the TC-CP series, such Brønsted sites should be associated to chromium, as they are not observed for the bare supports, and their concentration increases as the chromium content increases.

When the samples are outgassed at increasing temperatures (Fig. 3) the band originated by the δ_s mode is clearly split, due to the presence of different types of Lewis surface sites on the surface. The bands are not removed even at the highest outgassing temperature (573 K). As above, the band due to ammonium species (i.e., ammonia adsorbed on surface Brønsted acid sites) is removed more easily, and, as with the TC-CP samples, all bands are removed at a lower temperature than that required for the unloaded support (3). This means that incorporation of chromium ions in some way decreases the strength of the surface Lewis acid sites.

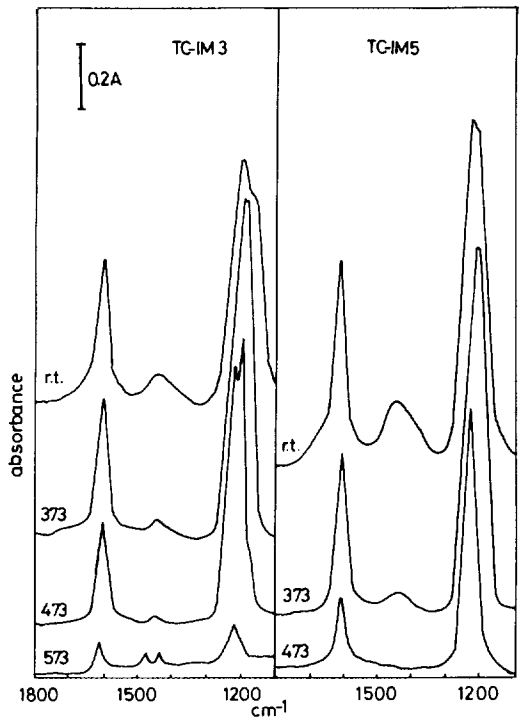

FIG. 3. FTIR spectra recorded upon adsorption of ammonia at room temperature on samples TC-IM3 and TC-IM5, and outgassing for 30 min at the temperatures given (K).

In order to investigate the nature of these surface sites, the samples were equilibrated with water vapour and then outgassed at room temperature before adsorption of ammonia. In this case, however, no change in the intensity of the band at 1446 cm^{-1} has been observed, if compared with that in the spectra recorded upon adsorption of ammonia on the dry sample, suggesting that no increase in the concentration of Brønsted sites is achieved by the treatment with water vapour.

The most informative band recorded upon adsorption of ammonia on the samples, with respect to the ability of surface Lewis acid sites to adsorb ammonia (i.e., about the strength of the surface Lewis acid sites), is that corresponding to the symmetric deformation mode, δ_s, of coordinated ammonia, recorded at 1300–1100 cm^{-1}. Its position has been related to the strength of the surface Lewis acid sites (11–13). So, if the results obtained here are compared to those reported in previous studies (14, 15), the following variation in surface acidity can be found:

$$WO_3/TiO_2 > MoO_3/TiO_2 > Cr_2O_3/TiO_2 > Fe_2O_3/TiO_2.$$

XPS Study

The binding energies corresponding to Ti(2*p*), O(1*s*), and Cr(2*p*) peaks, the full width half maxima (FWHM), the O/Ti intensity ratios, and the relative amount of oxygen present as OH^- and $O^=$, as obtained by deconvolution of the O(1*s*) peak, are listed in Table 1. The binding energies

TABLE 1

Ti(2*p*), O(1*s*), and Cr(2*p*) Binding Energies (eV) and XPS Intensity Ratios of TiO_2(P25) and TiO_2(hp), and of Catalysts (TC-IM) Prepared by Impregnation and Catalysts (TC-CP) Prepared by Coprecipitation Methods

	Ti($2p_{3/2}$)	Ti($2p_{1/2}$)	O(1*s*) ($O^=$)	O(1*s*) (OH^-)	Cr($2p_{3/2}$)	$OH^-/O^=$	O(1*s*)/Ti($2p_{3/2}$)[a]
TiO_2(P25)	458.8	464.5	530.1	531.8		0.16	2.7
	(1.4)	(2.2)	(1.3)	(1.3)			
TiO_2(*hp*)	458.9	464.5	530.5	531.5		0.02	2.5
	(2.0)	(2.6)	(2.2)	(2.2)			
TC-IM5	458.6	464.2	529.9	531.8	577.1	0.14	2.7
	(1.7)	(2.4)	(1.8)	(1.8)	(2.8)		
TC-IM3	458.7	464.4	530.0	532.0	577.3	0.14	2.8
	(1.5)	(2.3)	(1.8)	(1.8)	(2.8)		
TC-CP5	458.3	463.9	529.7	531.3	576.8	0.12	2.7
	(1.8)	(2.5)	(1.9)	(1.9)	(2.8)		
TC-CP2	458.5	464.2	529.8	531.5	576.9	0.11	2.6
	(1.6)	(2.3)	(1.7)	(1.7)	(2.8)		
TC-CP1	458.5	464.2	529.9	531.3	576.8	0.08	2.4
	(1.4)	(2.3)	(1.5)	(1.5)	(2.8)		
TC-CP.5	458.6	464.0	529.7	531.3	577.4	0.06	2.3
	(1.4)	(2.2)	(1.6)	(1.6)	(3.2)		

Note. The FWHM (eV) are given in parentheses.

[a] The total area of the two O(1*s*) components is considered. The intensity ratios have been divided by the relative sensitivity factors.

listed in Table 1 are typical of TiO_2 (16) and Cr_2O_3 (17,18). The $Cr(2p_{3/2})/Ti(2p_{3/2})$ area ratio was difficult to measure owing to the overlap between a Ti(2*s*) shakeup satellite, $Ti(2s)_{sat}$, observed only in the oxide species and lying at about 13 eV on the high-energy side of the Ti(2*s*) and the Cr(2*p*) line. However, an estimate of the Cr(2*p*) peak area was obtained by measuring the Cr(2*p*) + $Ti(2s)_{(sat)}$ intensity and subtracting the $Ti(2s)_{(sat)}$ intensity value as estimated from the corresponding signal, measured on pure TiO_2 using the intensity of the $Ti(2p_{3/2})$ with a weight factor of 0.15.

In the TC-CP samples, the Ti(2*p*) peaks and the O(1*s*) components relative to $O^=$ species, are shifted by ≈ -0.4 eV with respect to the corresponding values for (hp); their FWHM are smaller than the corresponding FWHM in TiO_2(hp). The $OH^-/O^=$ ratio of the TC-CP catalysts increases significantly with respect to that of the pure oxide. Typical Cr(2*p*), Ti(2*p*), and O(1*s*) spectra are given in Figs. 4 and 5.

The Cr(2*p*) spectra of the TC-CP5 samples taken after 10 and 40 min of X-ray exposure are shown in Figs. 4a and 4b, respectively. The asymmetries on the high energy side of the $Cr(2p_{3/2})$ and the $Cr(2p_{1/2})$ components have been fitted with an additional doublet shifted about 3.5 eV from the main peak. According to its energy, these peaks arise from contributions of small amounts of Cr (VI) and from the Ti(2*s*) shake up satellite, which energy

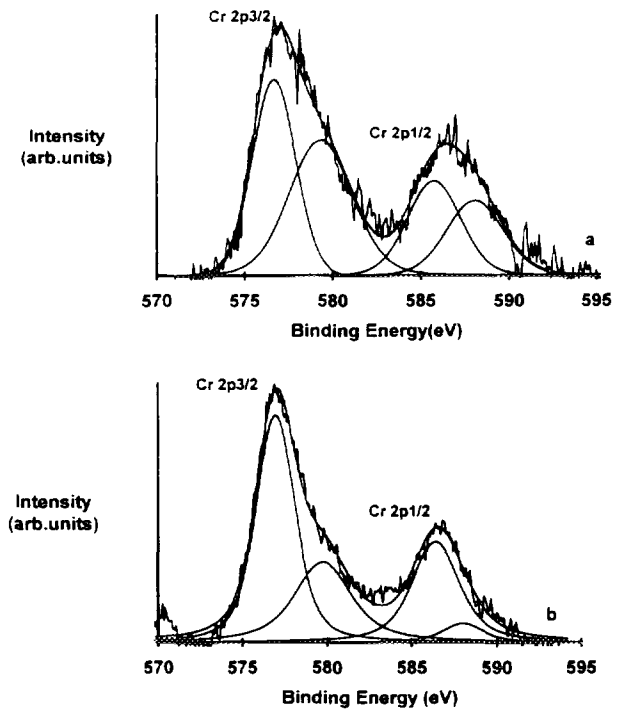

FIG. 4. Experimental and fitted Cr(2*p*) spectra of TC-CP5 sample after (a) 10 min and (b) 40 min of X-ray exposure.

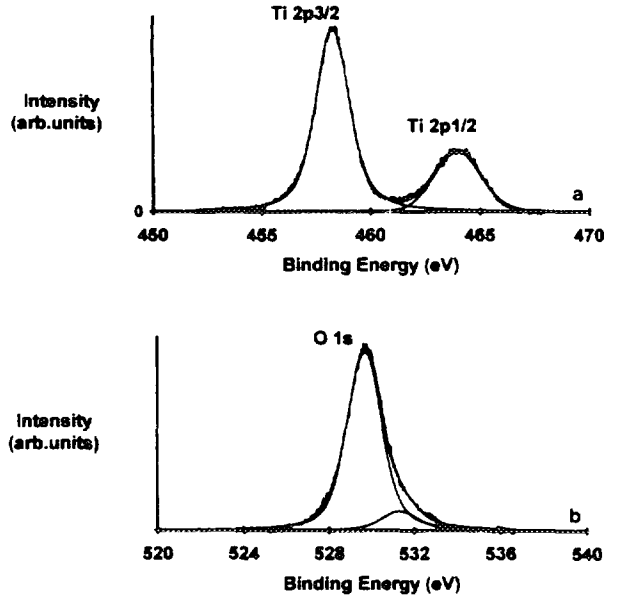

FIG. 5. Experimental and fitted Ti(2*p*) and O(1*s*) spectra of TC-CP5 sample.

and relative intensity have been determined in the Ti O_2(hp) sample. As was noticed in the most concentrated samples, exposure to the X-rays in the spectrometer chamber for more than 30 min decreased this high-energy component considerably and increased the Cr(III) component, suggesting reduction of Cr(VI) to Cr(III). The hexavalent state may have been produced by the preparation procedure of the catalysts, especially during the air firing at high temperature. After exposure to the X-rays, the Cr(VI) component decreases and the trivalent state increases. Similar photon-induced reduction of Cr(VI) during XPS analysis has been recently reported (19) in the case of electrochemically prepared films. The process was explained with the so-called "coulombic explosion" mechanism (20).

The oxidation state of chromium species supported on titania has been widely studied using different techniques. When supported on rutile, it has been shown by epr (21) that both Cr(III) and Cr(VI) species exist on the surface, despite the fact that Cr(III) or Cr(VI) precursor compounds were used to prepare the samples. Coupling between both species (Cr(VI)–Cr(III)–Cr(VI)) existing on the surface gives rise to average oxidation state of Cr(V). Upon calcination, migration along the *c* axis of the rutile structure leads to a decrease in the number of chromium species on the particle surface (22). This effect is less pronounced in the case of anatase because of the different structure of both phases (22).

The Ti(2*p*) spectrum is shown in Fig. 5a with the two spin orbit components. A negative chemical shift averag-

ing to ≈0.4 eV with respect to the TiO_2(hp) and slightly increasing with the chromium content is observed for the TC-CP samples. This shift may indicate a chemical interaction between the support and the dopant. It is difficult to explain the narrowing of FWHM, listed in Table 1, of TC-CP catalyst peaks with respect to the pure support, TiO_2(hp). Different morphology producing small differences in local charging may affect the widths.

The O(1s) signal shown in Fig. 5b for the TC-CP5 sample has two components: the high-energy component (531.3 eV) is attributed to OH^- and the low energy component (529.7 eV) to $O^=$. As indicated in Table 1, addition of chromium in the TC-CP samples, if compared to the pure TiO_2(hp), determines an increase of the OH^- component relative to the $O^=$ component. This result is in agreement with the presence of Brønsted acid sites (Cr–OH) detected by the FTIR study. Moreover, the XPS $OH^-/O^=$ ratios of the TC-IM samples and TiO_2(P25) are very close. The apparent disagreement with the infrared results, indicating the existence of Brønsted acid sites only in the Cr doped samples but not in the pure support, arises from the fact that the XPS technique reveals the total amount of OH groups present on the surface, whereas the IR results concern only those hydroxyl groups behaving as Brønsted acid sites. Therefore, it may be suggested that in TiO_2 P25 most of the hydroxyl groups are not activated as Brønsted sites.

Measurements of two different take-off angles were performed. Since no significant difference was observed, the average of the peak intensity results was used for the following analysis. In Fig. 6, the surface atomic concentrations, calculated from the Cr(2*p*) and Ti(2*p*) peak areas divided by their sensitivity factors, are plotted vs the nominal Cr/Ti atomic ratios. It is worth noting that for the TC-CP samples with Chromiumn contents up to 1% the XPS atomic ratios reflect the nominal concentration, whereas above 1% the surface atomic ratios are much larger than the nominal ones. The two impregnated samples exhibit the largest deviation.

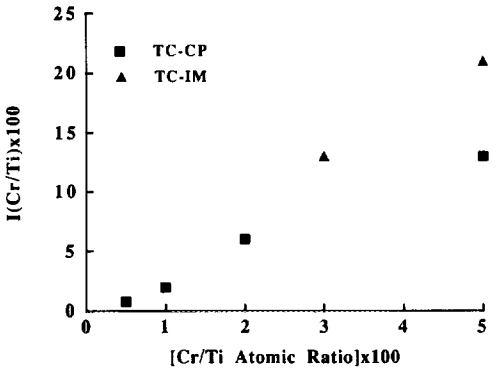

FIG. 6. Plot of XPS atomic ratios $I_{Cr/Ti}$ vs nominal Cr/Ti atomic ratio for the TC-CP and TC-IM series.

To relate the experimental intensity ratio to the surface Cr distribution, the model developed by Kerkhof and Moulijn (23) has been applied. According to this model, the catalyst consists of sheets of support, with cubic crystallites of dimension *c* in between. The thickness *t* of these sheets can be estimated from the density ρ and from the specific surface area of the support S_O according to

$$t = 2/\rho S_O. \quad [1]$$

The model assumes that the electrons leave the sample only in a direction perpendicular to the surface. Since the kinetic energies of the Cr($2p_{3/2}$) and Ti($2p_{3/2}$) photoelectrons are close, the mean free path, λ, of the different photoelectrons in the two media, TiO_2 and Cr_xO_y, are considered to be the same. According to this model, the intensity ratio in the case of crystallite formation is given by

$$(I_p/I_s) = (p/s)_b(\sigma_p/\sigma_s)\beta/2[(1 + e^{-\beta})/(1 - e^{-\beta})][(1 - e^{-\alpha})/\alpha], \quad [2]$$

where $(p/s)_b$ is the bulk atomic ratio of the promoter and support, σ are the photoelectron cross sections of the promoter and support XPS lines, λ is the mean free path of the analysed electrons, and β and α are the dimensionless sizes of the support thickness and of the crystallites given by

$$\beta = t/\lambda \quad [3]$$

$$\alpha = c/\lambda. \quad [4]$$

In the case of uniform monolayer catalysts the intensity ratio is given by

$$(I_p/I_s) = (p/s)_b(\sigma_p/\sigma_s)\beta/2(1 + e^{-\beta})/(1 - e^{-\beta}). \quad [5]$$

Equation 5 for monolayer catalysts has been used to calculate the Cr($2p_{3/2}$)/Ti($2p_{3/2}$) intensity ratios. The nominal concentration ratios, λ = 2 nm, according to the empirical formula for inorganic compounds (24), the Scofield cross sections, and the ρ and S_O appropriate to the Ti O_2(*hp*) and TiO_2 P25 (3) of the two series of samples, have been used. The predicted and the experimental intensity ratios versus the Cr/Ti atomic ratios for the TC-CP and TC-IM samples are reported in Fig. 7. The experimental values for the TC-CP series follow the theoretical prediction quite closely up to 2% Cr, differently from the TC-IM series, where the experimental values are consistently larger than the calculated ones.

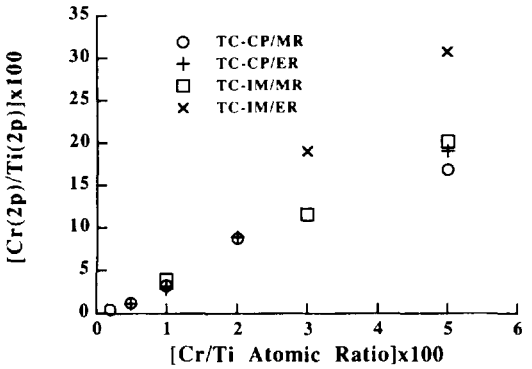

FIG. 7. Calcualted (according to the monolayer model, MR) and experimental (ER) intensity ratios of $Cr(2p_{3/2})/Ti(2p_{3/2})$ of TC-CP and TC-IM samples.

The comparison between the calculated curve and the experimental data in Fig. 7 for samples TC-CP suggests that the catalyst obtained by coprecipitation can be described by the monolayer catalyst model at least up to 2% chromium concentration. Above this concentration segregation phenomena may occur. Negative deviation from the monolayer line would have indicated formation of a discrete chromium phase, and this is not the case. This result is in agreement with the X-ray diffraction analysis, which excluded formation of Cr_2O_3 crystallites (2). The monolayer model does not apply to the impregnated catalysts (TC-IM), at least in the range of concentrations here studied. In this case, as it appears from Fig. 6, most of the chromium is concentrated on the outside of the titania particles resulting therefore in a large increase of the intensity ratio. A further addition of chromium ions would completely hide the titanium signal. It is likely that during the catalyst preparation the calcination temperature was too low to allow diffusion of chromium ions inside the titania lattice.

CONCLUSIONS

The results found in the present study indicate that in the Cr_2O_3/TiO_2 samples, whichever preparation method is used, two types of surface acid sites are present: Lewis sites and Brønsted sites. These last should be associated to the presence of chromium, as they do not exist in the unloaded supports, in particular to the presence of chromium ions in a high oxidation state, i.e., Cr(VI) (11). On the other hand, the Brønsted sites were not detected in a previous study carried out following the adsorption of pyridine on samples TC-CP (3). This difference is due to the higher basicity of ammonia than pyridine and to its lower size, thus making ammonia more adequate to "distinguish" between similar surface acid sites.

The XPS results have shown that both series of samples prepared by different procedures contain a certain amount of Cr(VI) which disappears during the XPS analysis due to a photoreduction process.

The analysis of the O(1*s*) peak indicated that addition of Cr to titania in the TC-IM samples does not change the relative amount of OH groups, whereas in the TC-CP samples as compared to the TiO_2(*hp*), the amount of the OH groups increases.

The catalysts prepared by coprecipitation, within 2% of chromium concentration, are well described by the model of monolayers of supported element uniformly distributed through the matrix of titania. The catalysts prepared by impregnation cannot be described by the same model because it appears that Cr builds up on the surface owing to the slow diffusion of Cr ions through the titania bulk. For the concentrations analysed no evidence of Cr_2O_3 crystallites exist, in agreement with the X-ray diffraction studies.

ACKNOWLEDGMENTS

A. M. V., L. P., and M. S. thank the Consiglio Nazionale delle Ricerche (CNR) and the Ministero dell'Universitá e della Ricerca Scientifica e Tecnologica (MURST) for financial support. I. M. acknowledges a grant from DGICYT (Madrid, Spain). Valuable help from Dr. A. Rossi (Universitá di Cagliari, Italy) and Dr. G. Mattogno (CNR, Roma, Italy) is also acknowledged.

REFERENCES

1. Borgarello, E., Kiwi, J., Graetzel, M., Pelizetti, E., and Visca, M., *J. Am. Chem. Soc.* **104,** 2996 (1982).
2. Palmisano, L., Augugliaro, V., Sclafani, A., and Schiavello, M., *J. Phys. Chem.* **92,** 6710 (1988).
3. Martin, C., Martin, I., Rives, V., Palmisano, L., and Schiavello, M., *J. Catal.* **134,** 434 (1992).
4. Criado, J. J., Macias, B., and Rives, V., *React. Kinet. Catal. Lett.* **27,** 313 (1985).
5. Seah, M. P., *SIA, Surf. Interface Anal.* **14,** 488 (1989).
6. Shirley, D. A., *Phys. Rev. B* **5,** 4709 (1972).
7. Sherwood, P. M. A., *in* "Practical Surface Analysis" (D. Briggs and M. P. Seah, Eds.), Appendix 3, p. 445. Wiley, New York, 1983.
8. Scofield, J. H., *J. Electron Spectrosc. Relat. Phenom.* **8,** 129 (1976).
9. Reilman, R. F., Msezane, A., and Manson, S. T., *J. Electron Spectrosc. Relat. Phenom.* **8,** 389 (1976).
10. Busca, G., Sausey, H., Saur, D., Lavalley, J. C., and Lorenzelli, V., *Appl. Catal.* **14,** 245 (1985).
11. Davydov, A. A., "Infrared Spectroscopy of Adsorbed Species on the Surface of Transition Metal Oxides." Wiley, New York, 1990.
12. Nakamoto, K., "Infrared and Raman Spectra of Inorganic and Coordination Compounds," 4th. ed. Wiley, New York, 1986.
13. Tsyganenko, A. A., Pozdnyakov, D. V., and Filimonov, V. N., *J. Mol. Struct.* **29,** 299 (1975).
14. del Arco, M., Martin, C., Rives, V., Sanchez-Escribano, V., Ramis, G., Busca, G., Lorenzelli, V., and Malet, P., *J. Chem. Soc., Faraday Trans.* **89,** 1071 (1993).
15. Martin, C., Martin, I., Rives, V., Palmisano, L., Schiavello, M., and Sclafani, A., *Catal. Lett.*, in press.

16. Slinkard, W. E., and De Groot, P. B., *J. Catal.* **68,** 423 (1981).
17. Wagner, C. D., Riggs, W. M., Davis, L. E., Moulder, J. F., and Muilberg, G. E., "Handbook of X-ray Photoelectron Spectroscopy." Perkin–Elmer, 1978
18. Petkov, K., Krastev, V., and Marinova, Ts., *SIA, Surf. Interface Anal.* **18,** 487 (1992).
19. (a) Okamoto, Y., Fujii, M., Imanaka, T., Teranishi, S., *Bull. Chem. Soc. Jpn.* **49,** 859 (1976); (b) Halada, G. P., and Clayton, C. R., *J. Electrochem. Soc.* **138,** 2921 (1991).
20. Cazaux, J., *Appl. Surf. Sci.* **20,** 457 (1985).
21. Evans, J. C., Relf, C. P., Rowlands, C. C., Egerton, T. A., and Pearman, A. J., *J. Mater. Sci. Lett.* **4,** 809 (1985).
22. Amorelli, A., Evans, J. C., Rowlands, C. C., and Egerton, T. A., *J. Chem. Soc., Faraday Trans. 1* **83,** 3541 (1987).
23. Kerkhof, F. P. J. M., and Moulijn, J. A., *J. Phys. Chem.* **83,** 1612 (1979).
24. Seah, M. P., and Dench, W. A., *SIA, Surf. Interface Anal.* **1,** 2 (1979).